



## Modeling and simulation in dynamic mode of a triple effect desalination system coupled to a plane solar collector

Ousmane Sow<sup>a,d</sup>, Thierry Maré<sup>b</sup>, Jamel Orfi<sup>c,\*</sup>, Mamadou Adj<sup>d</sup>

<sup>a</sup>Laboratoire de Matériau Mécanique et Energétique (LMME), Ecole Polytechnique de Thiès (EPT), Université Polytechnique de Thiès (UPT), Sénégal

<sup>b</sup>Laboratoire de Génie Civil et de Génie Mécanique (LGCGM), INSA de Rennes, IUT Saint Malo, 35043 Rennes, France

<sup>c</sup>Mechanical Engineering Department, College of Engineering, King Saud University, PO Box 800, Riyadh, 11421, KSA  
email: orfij@ksu.edu.sa

<sup>d</sup>Laboratoire d'Energétique Appliquée de l'Ecole Supérieure Polytechnique (ESP), Université Cheikh Anta Diop (UCAD) de Dakar Sénégal

Received 30 October 2009; Accepted 4 March 2010

---

### ABSTRACT

In traditional solar desalination stills, operating by phase change, a profitability problem exists, because the quantity of produced fresh water is rather small (3 to 4 liters per day per square meter of collecting surface). This article gives an account, via numerical simulation, of the time evolution of the various parameters and variables characterizing a triple effect system functioning on solar energy. It also gives an idea of the evolution of produced fresh water, brine discharge, and feed flowrate, and thus highlights the improvement of the daily water production per square meter. This simulation also shows the influence of the presence of salt on the thermodynamic characteristics of salt water solutions. Finally, a system of regulation of feed flowrates makes it possible to control salinity and thus to avoid the filling of salt into components of the installation like heat exchangers. The modelling of the system presented in this study, is based on the conservation equations of mass and energy for the various components.

*Keywords:* Solar desalination; Thermodynamics; Dynamical mode; Multiple effects

---

### 1. Introduction

The desalination of water of the salted underground layer “of the islands of Saloum”, constitutes a national concern for the researchers in Senegal [1–2]. In order to find a solution with low cost energy to this problem, the Laboratory of Applied Energy (LEA) of the Polytechnic University of Dakar directed its research towards solar desalination. Thus the present study relates to a triple effect desalination system coupled to a plane solar collector. It initially shows the influence of the presence of salt on the thermodynamic characteristics of salt water and thereafter the temporal evolution of the essential quantities of the installation (flow rates of brackish water feed,

and of extracted fresh water and brine, and enthalpies at various locations) and finally the thermodynamic cycle of water, from its entry in the form of brackish water to its exit in the form of fresh water and brine. So the performance of this system can be appreciated.

Several works dealing with solar desalination have been carried out. L. Zhang [3] carried out an experimental study to determine the performance of a traditional system of desalination by spraying salted water on horizontal tubes. The study led to an average production varying from  $0.7 \text{ kg} \cdot \text{h}^{-1}$  to  $2.5 \text{ kg} \cdot \text{h}^{-1}$  according to the insulation which goes from  $0.25 \text{ MJ} \cdot \text{m}^{-2}$ , to  $3.25 \text{ MJ} \cdot \text{m}^{-2}$ . The operating temperatures are between  $60^\circ\text{C}$  and  $85^\circ\text{C}$ . The study of H. Müller-Holst [4] made it possible to determine on TRNSYS, the coefficient of heat transfer between the evaporator and the condenser, at

---

\*Corresponding author.

the time of brine recycling in a one = effect desalination system. This coefficient is not constant. It varies from 25 to 275  $W \cdot m^{-2}$ , for operating temperatures going from 20 to 100 °C. A. I. Kudish [5], by simulation on a solar system of desalination with recovery of the latent heat, by a thermal approach, reached a production of 11  $kg \cdot m^{-2}$  per day. The characteristic of this study is not only to take into account the exact size of the components, but also the evolution according to the time of the production of pure water. The study of S. Zeinab [6] related to a traditional system of desalination using a parabolic solar collector. It gives the evolution of the production of water during the day. This production reaches a maximum of 0.4l per day for a temperature of the coolant of 60°C. I W Eames [7] carried out a simulation in permanent mode, followed by an experiment on a system for simple effect using brine recirculation. The results of simulation are based on a thermodynamic approach.

The production obtained is of 6.35  $kg \cdot m^{-2}$  per day. H. Tanaka [8] presented a basin with high production of water comparatively with the traditional basin. The study also shows the temporal variation of the production of fresh water. M. Reali [9] also worked on a barometric solar distiller and carried out an analysis on a system with simple effect then on two stages of distillation. For the same production of water, i.e. 36  $m^3$  per day in 10 operating hours, the single stage required 93.5 arrays of solar collectors with 100 tubes of 0.9  $m^2$ , whereas the double stages required 61.5 arrays of solar collectors for the same type of collector. In other words, the day labourer production is estimated at 4.278  $l \cdot m^{-2}$  per day for the simple stage and at 6.504  $l \cdot m^{-2}$  per day for the double stages. Other works on solar desalination exist [10,11] but use a system with humidification and dehumidification.

Most authors are working on sea water desalination and are disinterested in salinity of brine rejected. This is because rejected salinity is close to the initial sea water salinity and they consider that the volume of sea water is so big that dilution is automatically efficient.

In our case we are interested in countries of Sahel where water is rare. In this case these countries are using initial water salinity around 1%. The goal is to save as much water as possible and to reject it only when salinity is around 5.5%.

Indeed, starting from certain salinity, there is a risk of crystallization of the solid particles of the components (exchanging, evaporators, condenser etc.). The solution of the problem generally consists in using chemical substances, to prevent the deposit of these salts on the components, but this process is sometimes expensive.

The solution presented in this presentation is:

- To highlight a system of regulation making it possible to avoid the filling with salt on the components of the desalination plants.
- To minimise lost energy.

For the last solution we adopt triple effect desalination system coupled to a plane solar collector. We neglected vacuum energy because we use jet pump system coupled with solar water pump.

The works listed here make it possible to locate the order of magnitude of our results obtained by simulation, while waiting for the validation by an experimental study under development.

## 2. Presentation of the system

As shown in Fig. 1, the salt water is pumped into the installation by pump  $P_1$ , at a temperature of  $\theta_1$  (point 1). It crosses successively the heater (point 2), then the  $V_{2,3a1}$  valve, before penetrating through the evaporator (point 3<sub>a1</sub>) at a temperature close to that of evaporation. It is then transformed into a state of liquid–steam mixture (point 5<sub>a1</sub>), due to the heat provided by the solar loop exchanger Ech 11/12, and to the “vacuum” reigning in tank  $A_1$ , which corresponds to the saturated vapor pres-

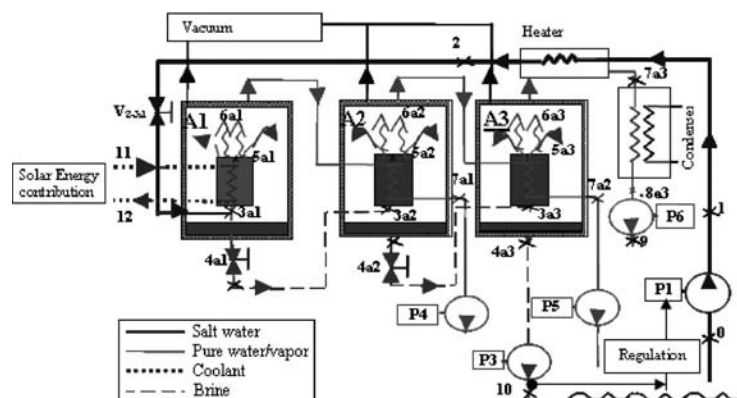


Fig. 1. Schematic representation of system under study.

sure  $p_{sat}^*$  of the raw material. The fluid vaporizes (point  $6_{a1}$ ). The brine (not evaporated water) extracted from the first enclosure (point  $4_{a1}$ ) is used to feed cell  $A_2$ , in the same way the vapour produced in the first  $A_1$  effect is used to vaporize salt water of the second effect  $A_2$ . In the same way, the brine resulting from the second effect  $A_2$  is used to feed the third effect  $A_3$  and the vapors produced in  $A_2$  are used to evaporate the water of tank  $A_3$ .

At the last stage, a condenser allows the passage into the liquid state of the vapors produced in the third effect.

### 3. Basic Equations

The equations modelling the system are based on the conservation equations for mass and energy in variable mode applied to each component of the installation (the evaporators, the condenser, the heater, the various valves, and various extraction pumps).

Throughout the study, the following positions apply:

- the presence of air in the fresh water production unit is neglected,
- the contributions of the kinetic and potential energy in the balance of total energy are also neglected,
- in insulated containers  $A_1, A_2, A_3$ , the thermal losses towards the outside are neglected,
- the vapor is supposed to be without salt,
- there is neither source nor sink of mass in the system.

Under these assumptions, the conservation equations of the mass and energy are expressed in their general form by Eq. (1), and Eq. (2):

$$f_s = f_f + f_b \tag{1}$$

$$\frac{d}{dt} [\mu]_{vc} + \Delta [f_s h]_{ec} = W' + Q' \tag{2}$$

The first two terms of Eq. (2) above concern the internal energy and the enthalpy of the medium. For these two quantities we determined their average values in the space of the control volume considered, by supposing that they obey a linear distribution.

By taking  $vc2$  as control volume (Fig. 2), and by neglecting energy losses through its walls, the assessment of energy is written:

$$m_{vc2,a1} \frac{du_{vc2,a1}}{dt} + f_{s,a1}(h_{5,a1} - h_{3,a1}) = Q'_{11/12} \tag{3}$$

Where  $m_{vc2,a1}$  represents the salt water mass contained in the evaporator of effect  $A_1$  (considered to be a constant) and  $u_{vc2,a1}$  the median value of specific internal energy in the space of  $vc2$  volume of effect  $A_1$ .

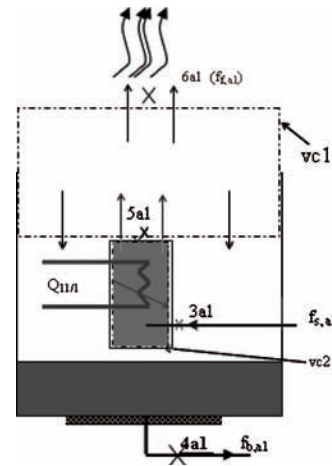


Fig. 2. Assessments of energy of the evaporator .

#### 3.1. Calculation of $\frac{du_{vc2,a1}}{dt}$

From the (p, h) diagram (Fig. 3) below, we have:

$$u_{vc2,a1} = u' + x_{a1}(u'' - u') \tag{4}$$

Indeed, taking into account the weak variations of enthalpy of the liquid saturated according to salinity will be compared to the vapor title  $x_{a1}$ . Thus

$$\frac{du_{vc2,a1}}{dt} = \frac{dx_{a1}}{dt} (u'' - u') \tag{5}$$

$$x_{a1} = \frac{h_{5,a1} - h'}{h'' - h'} \tag{6}$$

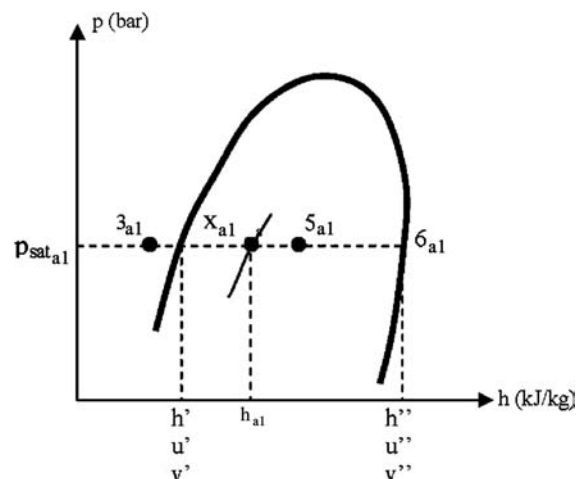


Fig. 3. Setting in evidence of the average title between  $3a_1$  and  $5a_1$ .

However

$$\frac{dx_{a1}}{dt} = \frac{dh_{5,a1}}{dt} \left( \frac{1}{h'' - h'} \right) \quad (7)$$

By replacing this result in Eq. (5), we obtain:

$$\frac{du_{vc2,a1}}{dt} = \left( \frac{u'' - u'}{h'' - h'} \right) \frac{dh_{5,a1}}{dt} \quad (8)$$

Knowing that:

$$\begin{aligned} u' &= h' - pv' \\ u'' &= h'' - pv'' \end{aligned}$$

Then

$$u'' - u' = (h'' - h') - p(v'' - v') \quad (9)$$

By taking into account Eq. (8), differential equation Eq. (3) becomes:

$$m_{vc2,a1} \left( \frac{u'' - u'}{Lv_{a1}} \right) \frac{dh_{a1}}{dt} + f_{s,a1}(h_{5,a1} - h_{3,a1}) = Q'_{11/12} \quad (10)$$

Then by replacing  $u'' - u'$  of Eq. (9) by its value in Eq. (10), we obtain:

$$\begin{aligned} m_{vc2,a1} \left( 1 - p_{sat,a1} \frac{v'' - v'}{Lv_{a1}} \right) \frac{dh_{a1}}{dt} \\ + f_{s,a1}(h_{5,a1} - h_{3,a1}) = Q'_{11/12} \end{aligned} \quad (11)$$

### 3.2. Calculation of $h_{a1}$

By supposing a linear space distribution along the ascending axis  $Y$  and uniform following  $X$  and  $Z$  of internal energy between sections  $3_{a1}$  and  $5_{a1}$  (Fig. 4), the median value of the enthalpy is expressed by:

$$h_{a1} = \frac{(h_{3,a1} + h_{5,a1})}{2} \quad (12)$$

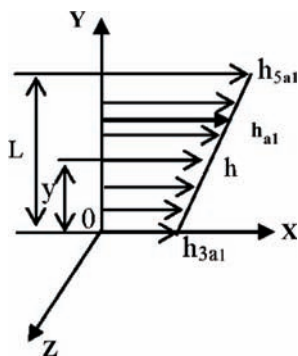


Fig. 4. Space distribution of energy interns between the points  $3_{a1}$  and  $5_{a1}$ .

### 3.3. Other equations of the model

Differential equation Eq. (3) then becomes

$$\begin{aligned} m_{vc2,a1} \left( 1 - p_{sat,a1} \frac{v'' - v'}{Lv_{a1}} \right) \frac{dh_{a1}}{dt} + 2f_{s,a1}(h_{a1}) \\ = Q'_{11/12} + 2f_{s,a1}h_{3,a1} \end{aligned} \quad (13)$$

With  $v' = \frac{1}{r^*(S_{sat,a1}T_{sat,a1}, p_{sat,a1})}$  and  $v''$ : given by thermodynamic table (steam).

$$\rho^*(S, T, p) = \frac{\rho(S, T, 0)}{\left[ 1 - \frac{p}{K(S, T, p)} \right]} \quad (14)$$

$\rho^*$  is given by the equation of state of the sea water [13] expressing the density according to  $S$ ,  $T$ , and  $p$ .  $\rho(S, T, 0)$  represents here the density for a null relative pressure, and  $K$  the module of compression given by Milero [13].

The solution of Eq. (13) gives us the evolution of  $h_{a1}$ , knowing that from the heat flow  $Q'_{11/12}$  according to time. We deduce  $h_{5,a1}$  starting from the expression of  $h_{a1}$  Eq. (12) knowing  $h_{3,a1}$ . By the same method, we obtain  $h_{5,a2}$  and  $h_{5,a3}$  by the resolution of equations Eq. (15) and Eq. (16) given below:

$$\begin{aligned} m_{vc2,a2} \left( 1 - p_{sat,a2} \frac{v'' - v'}{Lv_{a2}} \right) \frac{dh_{a2}}{dt} + 2f_{s,a2}(h_{a2}) \\ = Q'_{6,a1/7,a1} + 2f_{s,a2}h_{3,a2} \end{aligned} \quad (15)$$

$$\begin{aligned} m_{vc2,a3} \left( 1 - p_{sat,a3} \frac{v'' - v'}{Lv_{a3}} \right) \frac{dh_{a3}}{dt} + 2f_{s,a3}(h_{a3}) \\ = Q'_{6,a2/7,a2} + 2f_{s,a3}h_{3,a3} \end{aligned} \quad (16)$$

In addition, we neglected thermal inertia in the pumps, the valves, the heater, and the condenser, which amounts to not taking into account the non-stationary effects. The non-stationary effects are then considered only in the three cells of evaporation. Under these considerations, equations of energy on the components, other than the evaporators, are expressed with a semi-permanent mode, i.e. a succession of permanent modes at very short time intervals.

To these equations are added those given by:

– the equation giving the influence of the presence of salt on the enthalpy [14]:

$$h^*(S, T) = (D_1(S) + A_1(S) \cdot T + B_1(S) \cdot 10^{-4} \cdot T^2 + C_1(S) \cdot 10^{-6} T^3) \cdot 4.185 \quad (17)$$

$A_1(S), B_1(S), C_1(S), D_1(S)$  are polynomial functions of the second degree of the variable  $S$ .

– the equation giving the influence of salinity and of temperature on the saturation pressure [15]:

$$p_{sat}^*(S, T) = p_0(T) e^{\left[-1.106 \cdot 10^{-2} J(S) + 9.1673 \cdot 10^{-4} \cdot [J(S)]^2\right] \cdot \text{Ln}(10)} \quad (18)$$

Where  $J(S)$  is a polynomial function [15].

– The definition of the effectiveness of the various exchangers, expressed with the enthalpy at the entries and exits of points 1 and 2:

$$\varepsilon_{1/2} = \frac{h_2 - h_1}{h_{2\text{lim}} - h_1} \quad (19)$$

With  $h_{2\text{lim}}$  thermodynamic data starting from the diagram (p, h) (see paragraph 4, Fig. 15).

– The weight breakdown of salt in the evaporators:

$$S_{4,a1} = \frac{S_{3,a1}}{1 - x_{a1}} \quad (20)$$

Quantities of produced fresh water and rejected brine:

$$m_f = \int_{t_{ini}}^{t_{fin}} f_f dt \quad (21)$$

$$m_b = \int_{t_{ini}}^{t_{fin}} f_b dt \quad (22)$$

– The time dependence of the solar radiation flux is supposed to be given by a sinusoidal function over one insolation interval of 10 hours:

$$Q'_{11/12} = h_{sol} \times A \cdot I_{max} \sin p \left[ \frac{t - t_{ini}}{t_{fin} - t_{ini}} \right] \quad (23)$$

Taking into account all these equations brings us to a system of 35 equations with 36 unknown variables. The missing equation is given by the regulation:

$$\frac{Q'_{11/12}}{f_s} = C \quad (C = \text{constant}) \quad (24)$$

Constant  $C = 700 \text{ kJ} \cdot \text{kg}^{-1}$  is given in [12], following an analysis of the installation by energy and energetic analysis. Indeed, the object of the regulation is to avoid the risk of filling the components with salt on account of the strong salt concentrations. When the mass flow increases, the specific heat exchanged ( $q_{11/12}$ ) keeps a

Table 1  
Mass heat capacity of the salt water [2]

Mass heat capacity cp (J · kg <sup>-1</sup> · °C <sup>-1</sup> )						
P (bar)	Temperature (°C)					
	0	10	20	30	40	S
0	4048.4	4041.5	4044.8	4049.1	4051.2	1.5
100	4011.5	4012.9	4020.2	4026.9	4031.8	
0	4017.2	4013.8	4019.1	4024.7	4027.2	2.5
100	3982.1	3986.2	3995.4	4003.2	3990.8	
0	3986.5	3986.3	3993.9	4000.7	4003.5	3.5
100	3953.3	3959.9	3970.9	3979.7	3985.2	
0	3956.4	3959.3	3968.9	3977.0	4003.5	4.0
100	3925.0	3934.1	3946.8	3956.6	3985.2	

constant value, during all the regulation process. Under this consideration, constant  $C$  was given starting from an analysis of the system in steady state aiming at delimiting a zone of optimal regime [12]. For that, we expressed salinity as a function of the energy provided per kg of salted water treated, and noted that to a salinity of 5.5% correspond a value of the report/ratio  $q_{11/12} = \frac{Q'_{11/12}}{f_s}$  of:

- 1900 kJ · kg<sup>-1</sup> for a simple effect system
- 1000 kJ · kg<sup>-1</sup> for a double effect system
- 750 kJ · kg<sup>-1</sup> for a three effect system

which allows us to fix the value of constant  $C$  to 700 kJ · kg<sup>-1</sup>, with respect to the applicable zone defined by O. Sow [12] i.e.  $680 < C < 750 \text{ kJ} \cdot \text{kg}^{-1}$ .

In addition, table 1 shows that in our field of study ( $0.12 \text{ bar} < p_{sat}^* < 0.2 \text{ bar}$ ), the influence of pressure on the specific heat capacity  $cp^*$  is negligible, and consequently also on the enthalpy of the salt water  $h^*$ .

#### 4. Results

The present simulation concerns the time evolution of the following quantities: enthalpies at various points, various flow rates ( $f_s, f_b, f_f$ ), vapor title, and salinity. We considered for this simulation:

- a sinusoidal solar radiation flux with a maximum of 1 kW · m<sup>-2</sup> for an insolation interval of 10 hours
- a brackish water of an initial salinity of 1%, at a temperature  $\theta_1$  of 20°C
- a quantity of 20 liters of water in various tanks  $A_1, A_2, A_3$
- an exchanger (heater) of effectiveness 0.8
- a collecting surface of 25 m<sup>2</sup>

- a solar collector of efficiency 0.6
- a saturation temperature of 60°C in effect 1, 55°C in effect 2, and 50°C in effect 3.

The equations of the model being coupled, the method of resolution is thus numerical. Various differential equations (13), (15), and (16) resulting from the conservation equation of energy Eq. (3), were solved by the method of Runge Kutta of order 4–5. And for the determination of the quantities of produced and rejected water, we used a polynomial approximation of order 6–7, in order to calculate the time integrals Eq. (21, 22).

Simulation gives the following results then.

Figs. 5, 6, 7, and 8 show the temporal evolution enthalpy of the various points of the installation, and that of the vapor title for the various effects (cells  $A_1$ ,  $A_2$ ,  $A_3$ ). They thus make it possible to identify the state of the fluid in various places of the installation.

Figs. 9, 10, 11, 12 give indications on the temporal variation of the produced pure water and brine, rates of feed, that of salinity in the various effects. They thus make it possible to estimate the quantities of produced pure

water (table 2), and of brine rejected, with indications on the salinity of extraction of these rejections (Fig. 11). Table 2 shows in particular the percentages of water reject for the controlled and non-controlled systems. We compare our results with the various studies of the authors quoted to see the saving made on the water

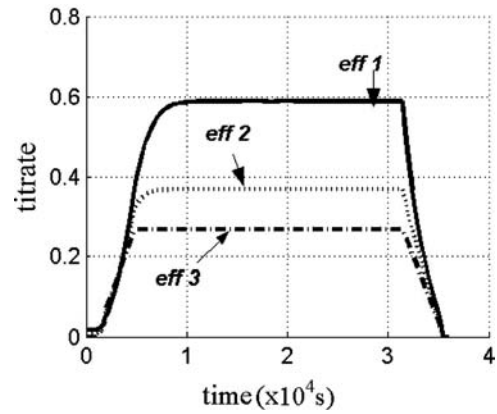


Fig. 7. Enthalpy of entering water.

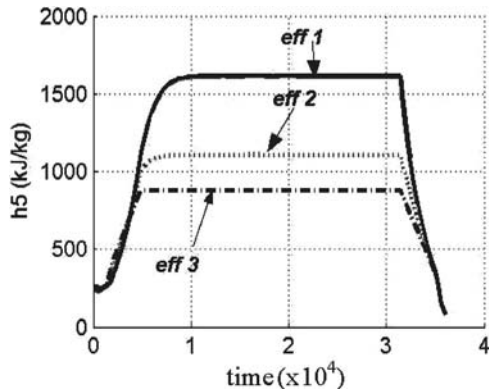


Fig. 5. Enthalpy of the liquid mixture-vapor in the various effects.

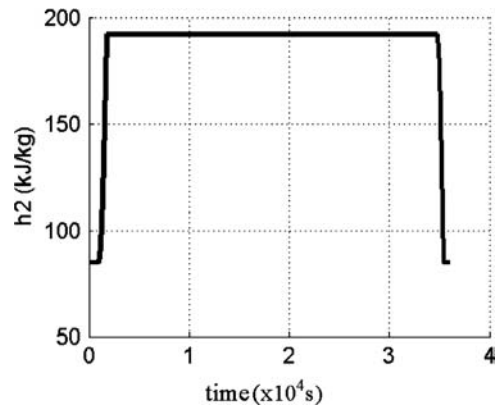


Fig. 8. Titrate-vapor in the different effects.

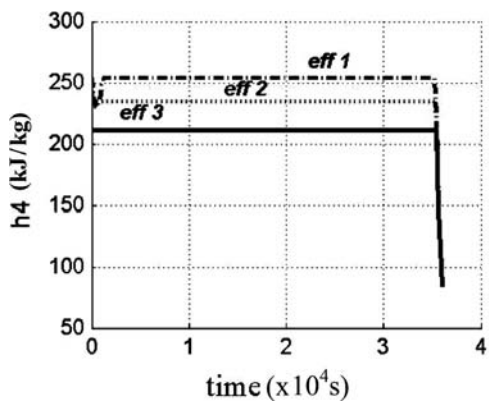


Fig. 6. Enthalpy of water at exit 4, in the various effects.

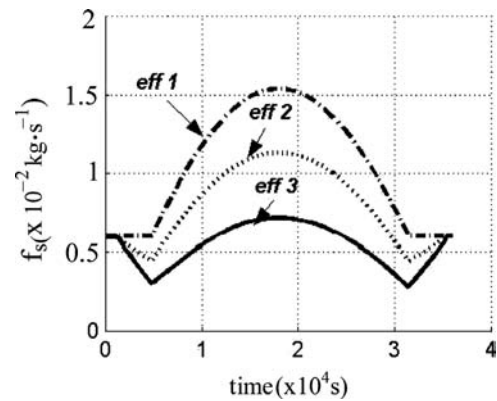


Fig. 9. Flow of feed water.

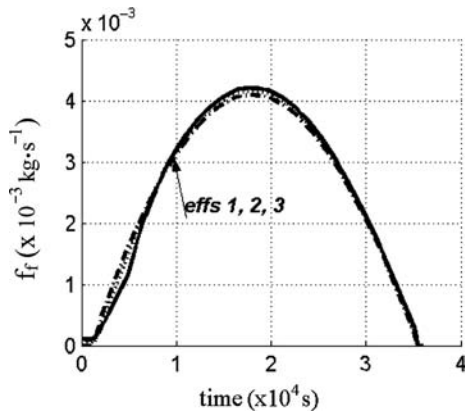


Fig. 10. Pure water flow in the various  $f_f$  effects.

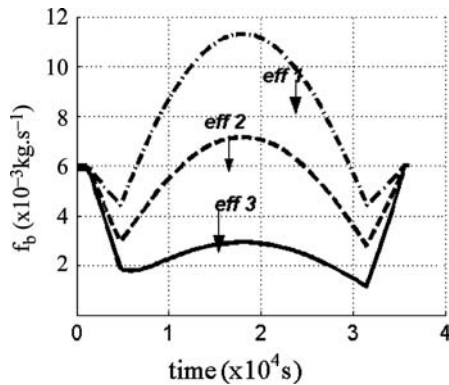


Fig. 11. Brine flow in different effects.

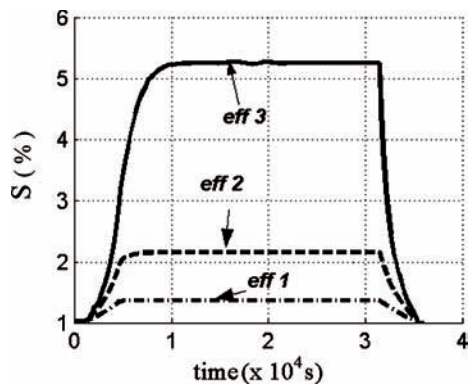


Fig. 12. Salinity in the various effects.

discharges. In general, as the results show, nobody is worried about the water discharges, because salt water exists with profusion in the sea. But for the desalination of brackish water in the countries of Sahel, water is rare and expensive. Hence it must be saved. It is thus necessary to give particular attention to the water discharges.

Figs. 13 and 14 show the influence of the presence of salt on the diagram of (p, h) of pure water. Indeed, taking into account equations Eqs. (17) and (18) in their field of validity, made it possible to plot the curves started in this diagram (p, h). Thus we note that the more the salinity (S), more the curve of pure water ( $S = 0\%$ )

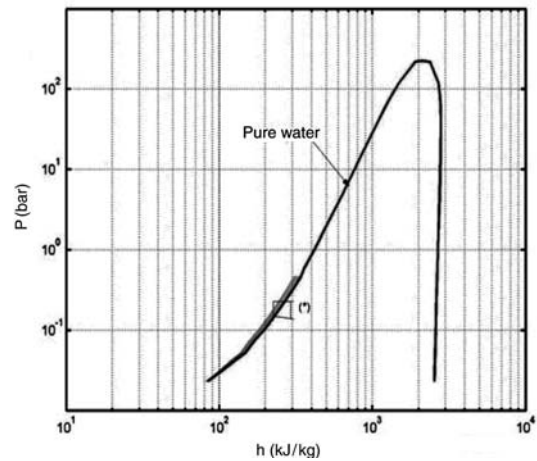


Fig. 13. Influence presence of salt on the diagram (p, h) of pure water.

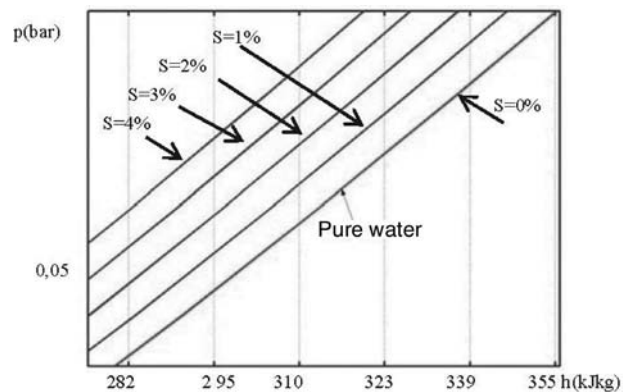


Fig. 14. Detail (\*) of figure 13.

Table 2

Production of pure water ( $r_f$ ) and brine Rejection ( $r_b$ ); \* Th.: theoretical study; Exp.: experimental study

	rej (%)	rep(%)	Prod (kg · m <sup>-2</sup> · day <sup>-1</sup> )	Observation results
Performance	23.7	76.3	15	In the present study (simulation)
Of systems	Upper then 90	Less then 10	7.9	*Th. And Exp. [7]
	71.2	28.8		Th. And Exp. [3]
	72.5	27.5	11	Th. And Exp. [5]

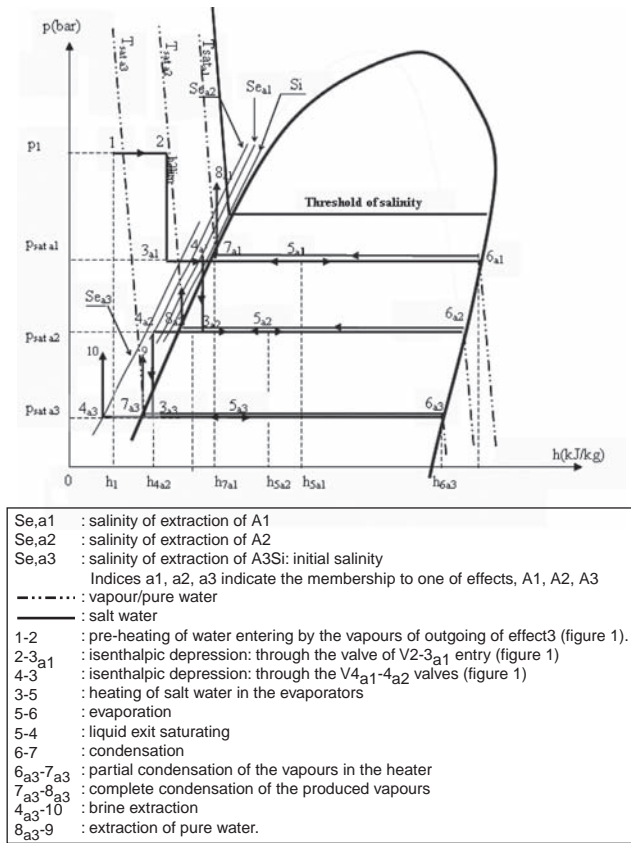


Fig. 15. Thermodynamic cycle of water during the process of desalination.

shifts towards the left, thus giving the curves for  $S = 1, 2, 3,$  and  $4\%$ .

Thus, on the assumption of a quasi-permanent mode, the thermodynamic cycle of water (at every moment) from its entry in the form of salt water until its extraction in the form of pure water on the one hand and of brine on the other hand is qualitatively given by Fig. 15.

**5. Conclusion**

This study gives an idea on the performance of a triple effect solar desalination system. Indeed, at the conclusion of this study we can say that this process constitutes an alternative for the developing countries. Its cost of realization is substantially reduced compared to the traditional multiple effect system [7], with the suppression of the boiler, and the reduction of the number of exchangers. The energy cost is also reduced with the use of solar energy. And finally the production passes from  $4 \text{ l} \cdot \text{m}^{-2}$  per day (for traditional solar desalination) to  $15 \text{ l} \cdot \text{m}^{-2}$  per day (for the studied system). While referring to table 2, the study also confirms the importance of regulating brackish water flow rates. Note however that

this model is not checked in experiments, and that this work of validation is in hand at Laboratories LEA of ESP of Dakar and LGCGM of the INSA of Rennes 1.

**Acknowledgements**

Our sincere thanks to Agence Universitaire pour la Francophonie, Colonel Mbarek DIOP of Senegal, Antoninon ZICHICHI of Switzerland, for the support brought to the Laboratory of Energy Applied (LEA) of ESP of DAKAR.

**Symbols**

- cp — specific heat at constant pressure,  $\text{kJ} \cdot \text{K}^{-1} \cdot \text{kg}^{-1}$
  - h — median value of specific enthalpy in the considered section,  $\text{kJ} \cdot \text{kg}^{-1}$
  - I — sunning,  $\text{W} \cdot \text{m}^{-2}$
  - L — length of control volume between points 3 and 5 in the effect A<sub>1</sub>, m
  - Lv — latent heat,  $\text{kJ} \cdot \text{kg}^{-1}$
  - m — mass of considered control volume, kg
  - p — pressure, Pa
  - prod — production of water,  $\text{kg} \cdot \text{m}^{-2} \cdot \text{day}^{-1}$
  - q — specific heat,  $\text{kJ} \cdot \text{kg}^{-1}$
  - Q' — thermal power, W
  - f — mass flow rate,  $\text{kg} \cdot \text{s}^{-1}$
  - rep — report/ratio of pure water recovery,  $\text{kg} \cdot \text{kg}^{-1}$
  - rej — brine rejection,  $\text{kg} \cdot \text{kg}^{-1}$
  - S — salinity, %
  - t — time, s
  - T — temperature, K
  - u — median value of specific internal energy in the space of vc volume,  $\text{kJ} \cdot \text{kg}^{-1}$
  - v — specific volume,  $\text{m}^3 \cdot \text{kg}^{-1}$
  - W' — mechanical power, W
  - X — titrate vapor,  $\text{kg} \cdot \text{kg}^{-1}$
  - (X, Y, Z) — coordinate of space
  - A — surface,  $\text{m}^2$
- Greek letters*
- ρ — density,  $\text{kg} \cdot \text{m}^{-3}$
  - θ — temperature, °C
  - ε — first law efficiency, %
  - η — energetic efficiency, %

**Component symbols**

- A — tank
- R — heater

V	—	valve
Ech i/j	—	Exchanging located between items i and j
P	—	pump

### Subscripts and superscripts

'	—	relative to a flow
*	—	relative to a brackish solution
0	—	relating to the ambient conditions
$a_i$	—	relating to effect $A_i$
b	—	brine
det	—	destroyed
ec	—	flow
f	—	fresh water
fin	—	final
(i/j)	—	component located between i and j
ini	—	initial
max	—	maximum value
ref	—	cooling
s	—	salted water
sat	—	relating to saturation
sol	—	relating to solar collector
sp	—	specific
vci	—	control volume n° i (i = 1,2,3,...)

### References

- [1] O. Sow, Analyse thermodynamique d'un système de dessalement par distillation avec apport solaire. Recherche des conditions optimales de fonctionnement en régime variable, Thèse de doctorat, Université de Valenciennes et du Hainaut – Cambrésis octobre, 2003.
- [2] O. Sow, B. Desmet, T. Mare and M. Adj, Modélisation et simulation en régime dynamique d'un système de dessalement à multiples effets couplés à un capteur solaire plan, VIIIème Colloque interuniversitaire Franco-Québécois sur la thermique des systèmes, Saint Malo, du 23–25 mai 2005.
- [3] L. Zhang, H. Zheng and Y. Wu, Experimental study on a horizontal tube falling film evaporation and closed circulation solar desalination system, *Renewable Energy*, 28 (2003) 1187–1199.
- [4] H. Müller-Holst, M. Engelhardt and W. Schölkopf, Small-scale thermal seawater desalination simulation and optimization of system design, *Desalination*, 122 (1999) 255–262.
- [5] A.I. Kudish, E.G. Evseev, G. Walter and T. Priebe, Simulation study on a solar desalination system utilizing an evaporator/condenser chamber, *Energy Conversion and Management*, 44 (2003) 1653–1670.
- [6] S. Zeinab, Abdel-Rehim and L. Ashraf, Experimental and theoretical study of a solar desalination system located in Cairo, Egypt, *Desalination*, 217 (2007) 52–64.
- [7] I.W. Eames, G.G. Maidment and A.K. Lalzad, A theoretical and experimental investigation of a small-scale solar-powered barometric desalination system, *App. Therm. Eng.*, 27 (2007) 1951–1959.
- [8] H. Tanaka, T. Nosoko and T. Nagata, A highly productive basin-type-multiple-effect coupled solar still, *Desalination*, 130 (2000) 279–293.
- [9] M. Reali, Solar barometric distillation for seawater desalting Part II: Analyses of one-stage and two-stage distillation technologies, *Desalination*, 190 (2006) 29–42.
- [10] M.B. Amara, I. Houcine, A. Guizani and M. Mâalej, Experimental study of a multiple-effect humidification solar desalination technique, *Desalination*, 170 (2004) 209–221.
- [11] E. Chafik, A new type of seawater desalination plants using solar energy, *Desalination*, 156 (2003) 333–348.
- [12] O. Sow, M. Siroux and B. Desmet, Energetic and exergetic analysis of a triple-effect distiller system driven by solar energy, *Desalination*, 174 (2005) 277–286.
- [13] M. Milero, C. Chen, A. Bradshaw and K. E. Schleicher, Oceanographic tables, Technical papers in marine sciences international, UNESCO, pp. 97, 1987.
- [14] Technical Data Book, Office of saline water, OSW 12–30, 1977.
- [15] L. Grumberg and M. Miles, Proceeding of the 3rd International symposium of fresh water from sea, 1970.